

## Original Research Paper

# Fuzzy PID-Inspired Potential Field Path Planning for Quadrotors in Environmental Monitoring

Mana Ghanifar<sup>1\*</sup> , Mobin Omidali<sup>2</sup> , AmirAli Nikkhah<sup>1</sup> , Mohammad Teshnehlab<sup>3</sup>, and Morteza Tayefi<sup>1</sup> 

1. Intelligent Control Systems Institute, K. N. Toosi University, Tehran, Iran

2. Malek-Ashtar University of Technology, Tehran, Iran

3. Faculty of Electrical Engineering, K. N. Toosi University of Technology, Tehran, Iran

## ARTICLE INFO

## ABSTRACT

**Article History:**

Received 06 August 2025

Revised 29 September 2025

Accepted 29 September 2025

Published Online 20 October 2025

**Keywords:**

Fuzzy adaptive potential field method

Quadrotor path planning

Environmental monitoring

Fuzzy logic

PID controllers

This paper introduces a novel approach for quadrotor path planning referred to as the Fuzzy PID-inspired Adaptive Potential Field Method (FPID-APFM). Traditional Potential Field Methods (PFMs) suffer from well-known limitations, including vulnerability to local minima, oscillations near obstacles, and the need for manual fine-tuning of control parameters, which can significantly degrade performance in complex or dynamic environments. To overcome these issues, the proposed FPID-APFM incorporates a fuzzy inference system that adaptively regulates key parameters in real-time, specifically the attractive force coefficient ( $k_a$ ) and the repulsive force coefficient ( $k_b$ ). This parameter adjustment mechanism is inspired by PID control concepts, where  $k_a$  plays a role analogous to the proportional gain ( $k_p$ ), directing the quadrotor toward its target, while  $k_b$  mimics the integral gain ( $k_i$ ), considering cumulative interactions with nearby obstacles and contributing to more stable and responsive navigation. Additionally, a damping factor ( $\zeta$ ) is introduced to reduce oscillations and ensure smoother trajectory generation, particularly in dynamic and cluttered scenarios involving moving obstacles. The method's effectiveness is validated through extensive simulation experiments conducted in both static and dynamic environments in MATLAB, including cases with wind disturbances and unpredictable changes. The results clearly demonstrate that FPID-APFM outperforms conventional approaches in terms of safety, smoothness, adaptability, and robustness. Overall, this method provides a reliable, flexible, and computationally efficient solution for real-world UAV navigation, package delivery, surveillance, search-and-rescue operations, and environmental monitoring.

\* Corresponding Author's E-mail: [managhanifar@email.kntu.ac.ir](mailto:managhanifar@email.kntu.ac.ir)

**How to Cite this Article:**

M. Ghanifar, M. Omidali, A. Nikkhah, M. Teshnehlab, and M. Tayefi, "Fuzzy PID-inspired potential field path planning for quadrotors in environmental monitoring," *Journal of Technology in Aerospace Engineering*, Vol. 9, Special Issue, pp. 1-12, 2025, <https://doi.org/10.22034/jtae.yyyy.nnnn>.

## COPYRIGHTS

Authors retain the copyright and full publishing rights.

Published by ARI. This article is an open access article licensed under the [Creative Commons Attribution 4.0 International \(CC BY 4.0\)](https://creativecommons.org/licenses/by/4.0/).



## 1 INTRODUCTION

Quadrotors have emerged as vital tools in various modern applications, such as package delivery, surveillance, search-and-rescue operations, and environmental monitoring. In environmental applications, quadrotors are increasingly utilized for tasks such as measuring air quality, collecting temperature gradients, and monitoring pollution levels. These tasks often require navigating through dynamic environments with obstacles like trees, buildings, and moving objects. Reliable and safe path-planning strategies capable of handling both static and dynamic obstacles are essential for effective environmental monitoring.

One widely recognized approach in robotic path planning is the Potential Field Method (PFM), initially proposed by Khatib [1]. This method defines navigation by considering the target as an attractive force and obstacles as repulsive forces [2]. While PFM offers a straightforward framework, it faces challenges such as local minima, oscillatory behavior near obstacles, and a lack of flexibility to adapt to complex and dynamic real-world scenarios [3]. To resolve the limitations of the traditional PFM, researchers have proposed various enhancements. For instance, some studies have modified the repulsive force equations to improve obstacle avoidance. An example of this is the work by Ge and Cui, who introduced a new PFM in dynamic environments, adjusting the repulsive forces to better handle moving obstacles [4]. Additionally, integrating PFM with optimization algorithms has been explored to adapt to changing conditions. For example, a fusion pathfinding algorithm combining an optimized A-star algorithm with the artificial PFM has been proposed to enhance path-planning performance in complex environments [5]. In recent years, fuzzy logic has shown capability in enhancing the robustness of PFMs. By using rule-based reasoning, fuzzy logic provides a flexible framework that enables algorithms to adapt more effectively to uncertainties and variations in dynamic environments. Research efforts, including the works of Lin and Jou [4] and Zhao et al. [5], have demonstrated the ability of fuzzy logic to

improve robot navigation. These studies show how fuzzy logic can overcome common challenges in traditional PFMs, making it a valuable tool for navigation in complex scenarios. In recent years, fuzzy logic has shown up as a promising approach to enhance the robustness of PFMs. Using rule-based reasoning, fuzzy logic enables algorithms to adapt more effectively to environmental uncertainties and dynamic variations. For example, the work of Wang [6] demonstrates the potential of fuzzy logic to improve robot navigation by overcoming critical challenges such as local minimum. Planning paths for quadrotors presents challenges that extend well beyond those faced by ground robots. Quadrotors navigate three-dimensional spaces and must comply with strict dynamic constraints, such as limits on lateral acceleration, to ensure their paths are both safe and practical. If these constraints are not considered, the result can be unsafe maneuvers or paths that are infeasible in real-world operations. While recent research has made progress in incorporating quadrotor dynamics into path-planning algorithms [7], many existing methods still struggle to solve the problem of real-world environments, particularly those involving dynamic obstacles. Recent studies have investigated the application of reinforcement Q-learning for fully autonomous optimal path planning in space robotics, highlighting its effectiveness in guiding docking and joint maneuvers during satellite servicing missions [8]. In parallel, a comprehensive body of research has focused on nature-inspired optimization algorithms for 3D trajectory planning in multi-UAV systems [9]. These algorithms have shown great potential in solving complex problems involving target assignment and coordinated tracking of multiple aerial targets, especially under dynamic and motion constraints. Such collective intelligence approaches provide robust solutions for enhancing the autonomy and efficiency of UAV swarms in mission-critical scenarios.

This paper presents an approach to solve these problems by introducing the Fuzzy PID-inspired Adaptive Potential Field Method (FPID-APFM). By dynamically adjusting the parameters of PFM using fuzzy logic, our approach takes inspiration from the PID control

rules, where the attractive and repulsive forces are treated similarly to the proportional and integral gains in that controller. This dynamic adjustment enables the quadrotor to navigate complex and changing environments more effectively. The method adapts the parameters, such as the attractive and repulsive force coefficients, in real-time, reducing the risk of getting stuck in local minima or oscillating near obstacles. Constraints like maximum lateral acceleration are also incorporated to ensure the generated paths are not only feasible but also smooth and safe for real-world operations.

This paper is organized as follows: Section 2 presents the quadrotor dynamics. Section 3 provides an overview of PFM and PID techniques. Section 4 introduces the proposed FPID-APFM, explaining its design, fuzzy rules, and parameter adaptation mechanisms. Section 5 details the simulation results in testing a real-world scenario. Section 6 shows the pseudocode of this simulation. Finally, Section 7 concludes the paper with a summary of findings and practical applications.

## 2 QUADROTOR DYNAMICS

The quadrotor represents a nonlinear system characterized by six degrees of freedom. Its dynamics are commonly modeled using the Newton-Euler formulation. These dynamics are typically categorized into translational and rotational components, reflecting the system's full range of motion [10]:

### 2.1 Translational Dynamics

The translational motion of the quadrotor in the inertial frame is given by:

$$m\ddot{\mathbf{r}} = \mathbf{F}_g + \mathbf{F}_t + \mathbf{F}_d \quad (1)$$

Here,  $\mathbf{r} = [x, y, z]^T$  denotes the position of the quadrotor in the inertial frame, while  $m$  represents the quadrotor's mass. The gravitational force is given by  $\mathbf{F}_g = [0, 0, -mg]^T$ , and the thrust force,  $\mathbf{F}_t = R[0 \ 0 \ T]^T$ , is expressed in the inertial frame using the rotation matrix  $R$ . Additionally,  $\mathbf{F}_d$  accounts for aerodynamic drag and any external disturbances.

### 2.2 Rotational Dynamics

The rotational motion of the quadrotor is described using the Euler angles  $\varphi$ (roll),  $\theta$ (pitch), and  $\psi$ (yaw):

$$I\dot{\boldsymbol{\omega}} + \boldsymbol{\omega} \times (I\boldsymbol{\omega}) = \boldsymbol{\tau} \quad (2)$$

Where  $\boldsymbol{\omega} = [p, q, r]^T$ ,  $I$  is the inertia matrix and  $\boldsymbol{\tau} = [\tau_\varphi, \tau_\theta, \tau_\psi]$  represents the control torques generated by the rotors.

### 2.3 Constraints on Quadrotor Dynamics

In real-world applications, quadrotors must operate within specific physical and operational limits to ensure their safety and functionality. These limits include restrictions on lateral acceleration, velocity, and roll angles, as well as the need to account for external factors like wind disturbances. This work considers the following key constraints:

#### 2.3.1 Thrust and Voltage Constraints

The total thrust generated by the rotors is limited by the maximum voltage supplied to the motors:

$$F_t \leq k_t V_{\max} \quad (3)$$

where  $V_{\max}$  is the maximum motor voltage, and  $k_t$  is the thrust coefficient. This ensures the generated forces remain within the hardware's operational limits.

#### 2.3.2 Lateral Acceleration Constraint

To ensure smooth and safe navigation, the lateral acceleration is limited:

$$a_{\text{lateral}} = \sqrt{a_x^2 + a_y^2} \leq a_{\max, \text{lateral}} \quad (4)$$

where  $a_{\max, \text{lateral}}$  is the maximum allowable lateral acceleration

#### 2.3.3 External Disturbances

Wind disturbances are modeled as forces acting along the  $x$ ,  $y$ , and  $z$  axes. These forces are randomly varied within a specified range to simulate real-world environmental conditions:

$$F_{wind} = [F_{wind,x}, F_{wind,y}, F_{wind,y}] \quad (5)$$

The impact of these disturbances is incorporated into the total forces acting on the quadrotor.

### 3 OVERVIEW OF PATH PLANNING AND CONTROL TECHNIQUES

#### 3.1 Potential Field Method

PFM is an important and functional approach in robotic path planning. The PFM at a specific point in the robot's configuration space is a scalar value derived from attractive and repulsive potentials. It considers the robot's environment as a field of forces, where the target acts as an attractive force pulling the robot toward it, while obstacles generate repulsive forces pushing the robot away. By reacting to the resulting force, the robot strives to move effectively toward its target while avoiding collisions.

In the Cartesian coordinate system, the robot's position is represented as  $q(x,y)^T$  [11]. So, the PF function can be stated as:

$$U(q) = U_{att}(q) + U_{rep}(q) \quad (6)$$

Where  $U(q)$ ,  $U_{att}(q)$  and  $U_{rep}(q)$  are the total potential field, attractive potential generated by the target and repulsive potential generated by obstacles, respectively.

The attractive field between the robot and the target is formulated to direct the robot toward the desired target area.

Where  $U(q)$ ,  $U_{att}(q)$  and  $U_{rep}(q)$  are the total potential field, attractive potential generated by the target and repulsive potential generated by obstacles, respectively.

The attractive field between the robot and the target is formulated to direct the robot toward the desired target area.

$$U_{att}(q) = \frac{1}{2} \times k_a \times (q - q_d)^2 = \frac{1}{2} k_a \rho_t^2 \quad (7)$$

$k_a$  is the positive attractive coefficient for PF and  $q_d$  is the current position vector of the

target.  $\rho_t$  is an Euclidean distance from the robot's location to the target location.

To ensure safe navigation, obstacles near the robot generate a repulsive force, pushing it away to prevent collisions. It should be noted that when obstacles are outside the defined range, they no longer influence the robot's movement, allowing it to focus on reaching the target. This behavior is mathematically represented by the repulsive potential function, which regulates the robot's motion based on its proximity to obstacles:

$$U_{rep}(q) = \begin{cases} \frac{1}{2} k_b \left( \frac{1}{d(q)} - \frac{1}{d_0} \right)^2 & d(q) \leq d_0 \\ 0 & d(q) > d_0 \end{cases} \quad (8)$$

$k_b$  is the repulsive coefficient.  $d$  and  $d_0$  are the distance between the robot and the obstacle and the distance of the obstacle's repulsive force field, respectively.

The total force acting on the robot, as shown in Fig. 1, comes from a combination of two components: the attractive and repulsive forces. The attractive force, calculated from the gradient of the attractive potential field, pulls the robot toward its target. On the other hand, the repulsive force, derived from the gradient of the repulsive potential field, pushes the robot away from obstacles. Together, these forces work to guide the robot's movement effectively [11].

$$F(q) = -\nabla U_{att}(q) - \nabla U_{rep}(q) \quad (9)$$

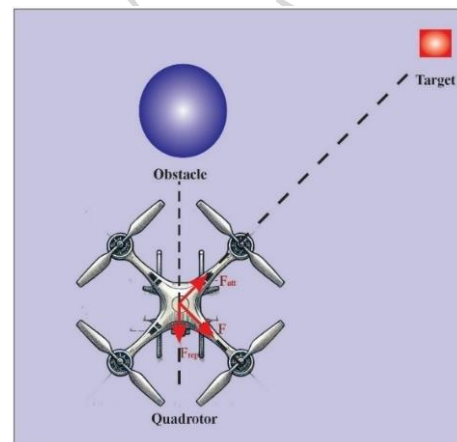


Fig. 1. Schematic illustration of the resultant force generated by the potential function for a quadrotor.

### 3.2 PID Control Method

PID control is a fundamental technique used in control systems to maintain desired outputs by adjusting control inputs based on the error between the desired and actual states of a system. The algorithm consists of three components: the Proportional (P) term, which produces an output proportional to the current error; the Integral (I) term, which accumulates past errors to eliminate steady-state error; and the Derivative (D) term, which responds to the rate of change of the error to counteract future error, thereby enhancing stability.

The weighting factors ( $k_p$ ,  $k_i$  and  $k_d$ ) of a PID controller can be adjusted to fine-tune its performance and achieve optimal system behavior.

$$CI(t) = k_p e(t) + k_i \int e(t) dt + k_d \frac{d}{dt} e(t) \quad (11)$$

CI is the output of the PID controller.  $k_p$ ,  $k_i$  and  $k_d$  are Proportional, Integral, and Derivative gains.

In this study, the control gains  $k_p$ ,  $k_i$  and  $k_d$  were adopted from the methods presented in [12], where these parameters were tuned to ensure both stability and fast convergence in similar dynamic conditions.

## 4 FUZZY POTENTIAL FIELD METHOD

PF method is widely used in robotic path planning, faces several limitations that can reduce its effectiveness, particularly in dynamic and real environments. One of its primary challenges is the need for precise parameter tuning, especially the values of the attractive and repulsive forces. In addition to these issues, PFM also struggles with problems such as getting stuck in local minima [9]. By adjusting parameters in real-time, fuzzy logic helps PFM better adapt to changing conditions and enhances its overall performance. **Fig. 2** illustrates the rule surface of a fuzzy inference system, depicting the relationship between two

inputs, the error and its derivative, and the three outputs.

In the prevention of potential singularities or abrupt changes in fuzzy gains, input and output spaces of the fuzzy inference system are normalized, and gain values are fixed with saturation limits. The rule base is also smoothed in variation and prevents abrupt changes, particularly at boundary conditions. It prevents destabilization or lag in any operating region.

### 4.1 $k_a$ , Attractive Coefficient

In PFM,  $k_a$  is crucial for influencing the robot's path and its approach to the target. Increasing  $k_a$  increases the attractive force, enabling the robot to move more quickly toward the target. Setting  $k_a$  too high may result in overshooting or oscillatory behavior, especially in dynamic environments. On the other hand, a lower  $k_a$  results in smoother and slower motion. This can be beneficial for precise navigation or when operating in areas with many obstacles.

The roles of  $k_p$  in a PID controller and  $k_a$  in the PF method are the same in concept because both parameters determine the strength of a system's response toward its target.

In a PID controller,  $k_p$  determines the intensity of the system's reaction to the difference between the current state and the desired value. A higher  $k_p$  accelerates the response to minimize the error but can create overshooting or oscillations if set too high. In contrast, a lower  $k_p$  results in a more stable response, though it may slow down convergence.

Thus, both  $k_p$  in a PID controller and  $k_a$  in the PF method make a trade-off between speed and stability. Increasing their values makes the system respond faster but comes with the risk of instability while lowering them improves stability but slows down progress.

### 4.2 $k_b$ , Repulsive Coefficient

In the PFM, the repulsive coefficient  $k_b$  plays a critical role in helping the quadrotor effectively avoid obstacles. A higher  $k_b$  increases the magnitude of the repulsive forces, allowing for stronger and more immediate responses to nearby obstacles. On the other hand, lowering  $k_b$  reduces the repulsive forces,

making the movement smoother and more direct.

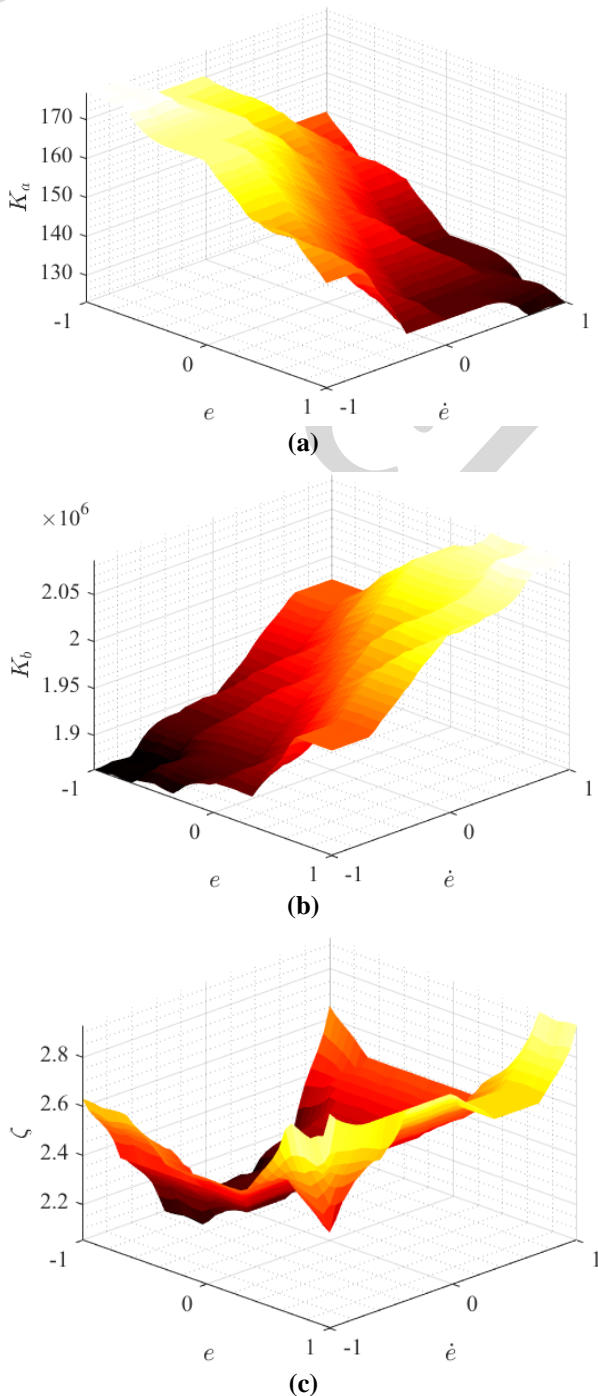


**Fig. 2.** Rule surface visualization of the fuzzy inference system (adapting from [13]) (a)  $k_a$ , (b)  $k_b$  and (c)  $\zeta$ .

However, this comes with the trade-off of a higher risk of collisions or not having enough clearance around obstacles.

The roles of  $k_i$  in a PID controller and  $k_b$  in the PF method share similarities in that both handle the effects over time  $k_i$  in error accumulation and  $k_b$  in obstacle avoidance.

In PID control,  $k_i$  corrects steady-state error by collecting past deviations from the desired value. A higher  $k_i$  helps eliminate steady-state error but can cause instability or oscillations if set too high. Similarly,  $k_b$  builds influence over the robot's path by continuously modifying its response based on the presence of obstacles.

Although the link between  $k_i$  and  $k_b$  isn't as straightforward as that between  $k_p$  and  $k_a$ , both parameters play a role in making long-term corrections.  $k_i$  does this by dealing with accumulated errors, while  $k_b$  ensures the robot avoids obstacles along its path.

### 4.3 $\zeta$ , Damping Factor

In our simulated PFM, the damping factor  $\zeta$  is responsible for controlling the rate of change of the robot's velocity, influencing how the robot slows down as it approaches its target or navigates around obstacles. In other words, it is used to scale the force applied to the robot. A higher  $\zeta$  results in a more damped response, reducing oscillations and overshooting, leading to smoother and more stable motion. However, if  $\zeta$  is set too high, the system converges too slowly, so affecting the overall performance. In contrast, a lower  $\zeta$  value reduces damping, allowing the robot to move more quickly toward the target, but this can increase the risk of instability, such as oscillations.

Similarly, in a PID controller,  $k_d$  determines how the system responds to the rate of change in the error signal.

It provides an effect to reduce overshoot and oscillations by accounting for how quickly the system is approaching the setpoint. A higher  $k_d$  value results in faster corrections by damping the system's response, helping to prevent overshoot. However, excessively high  $k_d$  values can lead to overcompensation.

In contrast, a lower  $k_d$  value produces quicker responses but may increase overshooting and system instability.

Therefore, both parameters help smooth the system's response, reduce oscillations, and ensure stability.

## 5 SIMULATION

**Fig. 3** illustrates a schematic representation of the proposed path-planning system for a quadrotor tasked with environmental monitoring in a real environment. The orange path represents the nominal path that the FPID-APFM is designed to generate. The generated path enables the quadrotor to safely navigate toward its target while avoiding obstacles. Dynamic obstacles, such as moving birds, are highlighted by red circles, demonstrating the algorithm's ability to dynamically adjust the path in real-time. Static obstacles, like trees or stationary structures, are indicated by blue circles. This figure emphasizes the algorithm's capability to handle both static and dynamic obstacles, ensuring the quadrotor collects environmental data efficiently and safely in real-world scenarios.

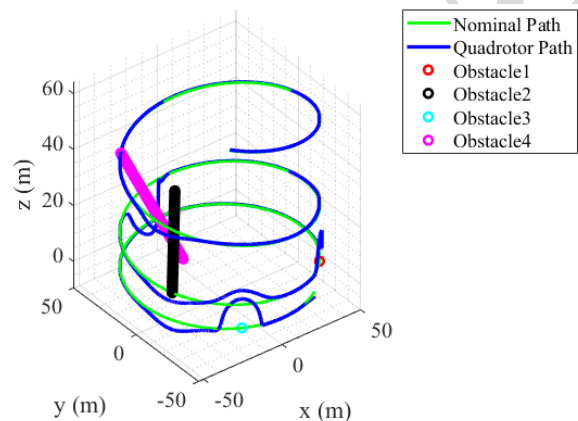


**Fig. 3.** Problem visualization (AI assisted).

**Fig. 4** represents the 3D simulation results of a quadrotor path-planning algorithm within a

cylindrical workspace. The environment contains a combination of static and dynamic obstacles, presenting a challenging scenario for safe navigation. The nominal path, shown in green, represents the path before considering environmental disturbances or obstacle interactions. The quadrotor path, depicted in blue, demonstrates the actual path followed by the quadrotor, reflecting its dynamic adjustments in response to obstacles and workspace constraints. The environment includes both static and dynamic obstacles. The static obstacles are represented by cyan and red points and remain fixed. In contrast, dynamic obstacles, shown in magenta and black, introduce an additional complexity as their positions change over time. The quadrotor's ability to avoid these moving obstacles while following the nominal path. In this simulation, the impact of wind on the path planning of quadrotors is modeled in three directions: X, Y, and Z. The wind values in each direction are simulated with a mean speed of 10 m/s and a variation factor.

Under the proposed method, a nominal trajectory is first created to steer the quadrotor in a general direction towards the target. The adaptive attractive policy, which is guided by the fuzzy PID-inspired potential field, subsequently modifies this trajectory dynamically in real time to counteract disturbances in the environment along with interactions with obstacles. In this architecture, the nominal path is a reference path and the attractive force actively drives the vehicle towards it, with flexibility to make flexible adjustments to enable collision-free and feasible navigation.



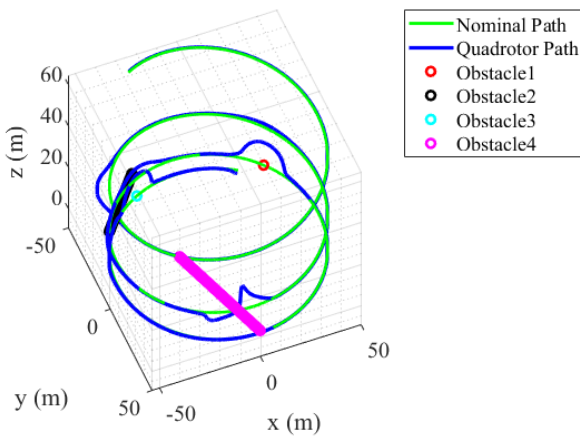
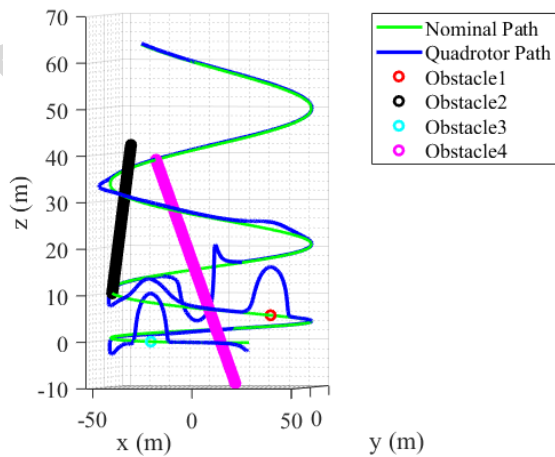


Fig. 4. Three different views of the 3D simulation illustrating the quadrotor's path planning.

Fig. 5 shows the velocity in all three axes, used to test the method's ability to adapt to wind forces in dynamic real-world conditions.

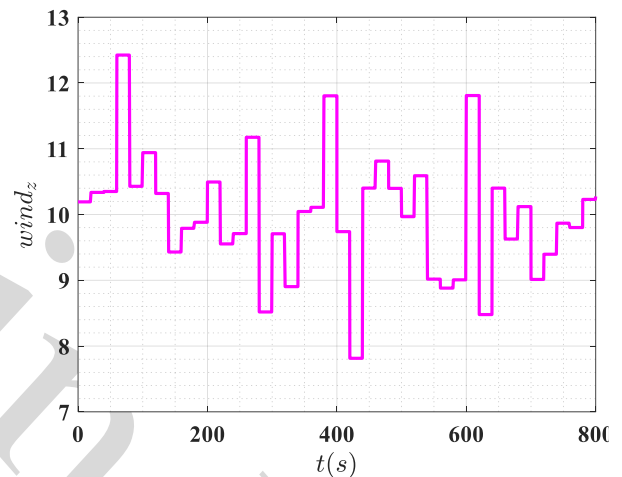
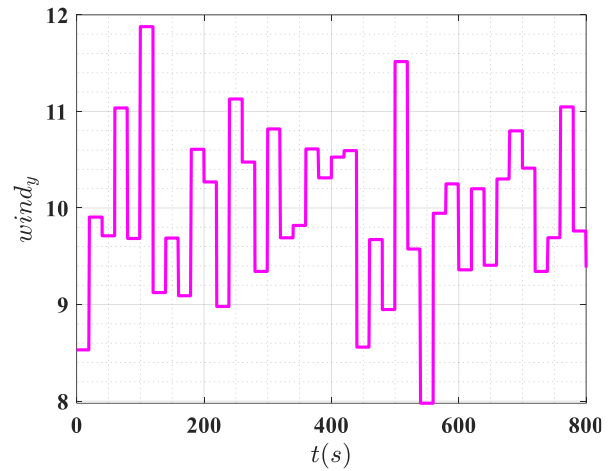
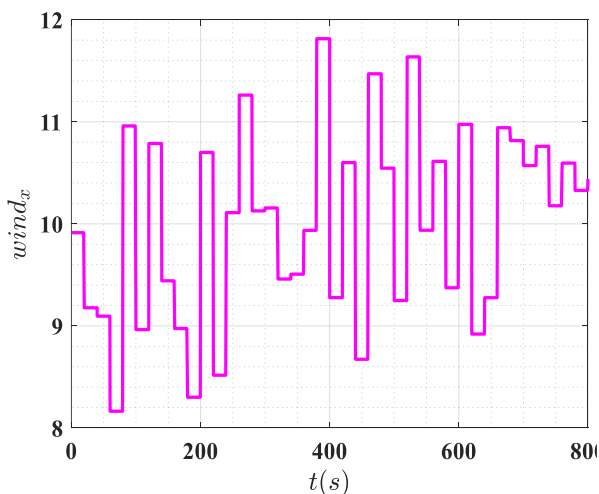


Fig. 5. Wind speed variation in the X, Y, and Z direction over time.

## 6 PSEUDOCODE

The pseudocode presented in Section 8 outlines the key steps of the algorithm, providing a clear understanding of the proposed method's functionality. It offers a detailed abstraction to ensure that the logic is practical for implementation.

## 7 CONCLUSION

This study introduces a path-planning method for quadrotors designed for environmental data collection in dynamic and complex real-world conditions. The approach uses PFM while overcoming its key challenges, such as instability near moving obstacles. By incorporating a fuzzy logic framework, the method enhances adaptability and decision-

making through its flexible, rule-based structure, making it more robust in uncertain scenarios. Practical considerations, such as lateral acceleration limits, are also integrated into the design to ensure safety and operational feasibility. Furthermore, the connection between PID control gains and potential field components highlights their shared behaviors and principles. The proportional gain ( $k_p$ ) aligns with the attractive force coefficient ( $k_a$ ) in PFM, driving the system toward its target. The integral gain ( $k_i$ ) corresponds to the path repulsive coefficient ( $k_b$ ), correcting steady-state errors over time for improved accuracy. Similarly, the derivative gain ( $k_d$ ) relates to the damping factor ( $\zeta$ ), which reduces oscillations and enhances stability. This analogy underscores the unified principles of control and optimization in both methods, providing a framework for developing reliable and accurate path-planning systems. Simulation results show the effectiveness of the proposed approach (FPID-APFM), demonstrating its ability to generate smooth, safe, and efficient paths. **Table 1** summarizes the correspondence between PID controller gains and PFM components, highlighting their respective applications.

**Table 1.** Mapping PID Gains to Potential Field Components and Their Applications.

Application	PF Coefficient	PID Gain
Determines the strength of the attractive force guiding the system toward its target.	$k_a$	$k_p$
Influences long-term corrective effects (obstacle avoidance vs. steady-state error correction).	$k_b$	$k_i$
Dampens oscillations and ensures the system remains stable.	$\zeta$	$k_d$

**Fig. 6, Fig. 7 and Fig. 8** illustrate the variation of the coefficients over a 800-second simulation. These figures show how the fuzzy inference system dynamically adjusts the attractive and repulsive force coefficients in response to the error and its derivative at each second. As clearly seen in the figures, the fuzzy rules continuously adapt the coefficients, reflecting the system's ability to fine-tune these parameters in real-time to ensure smooth path planning. This dynamic adjustment process is key to overcoming challenges such as oscillatory behavior and local minima, allowing the quadrotor to navigate more effectively in both static and dynamic environments.

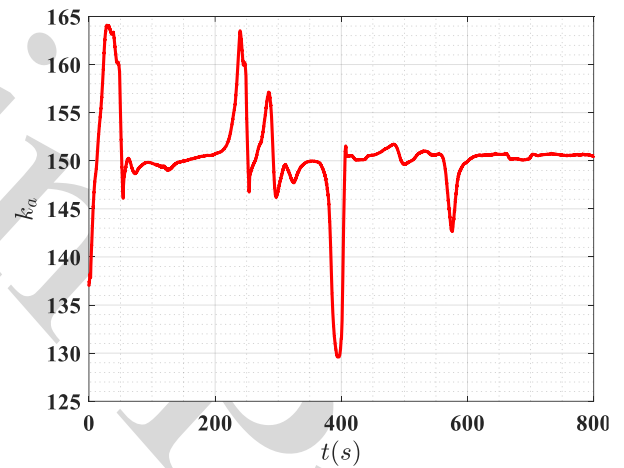


**Fig. 6.** The variation of  $k_a$  in the potential field method over time.

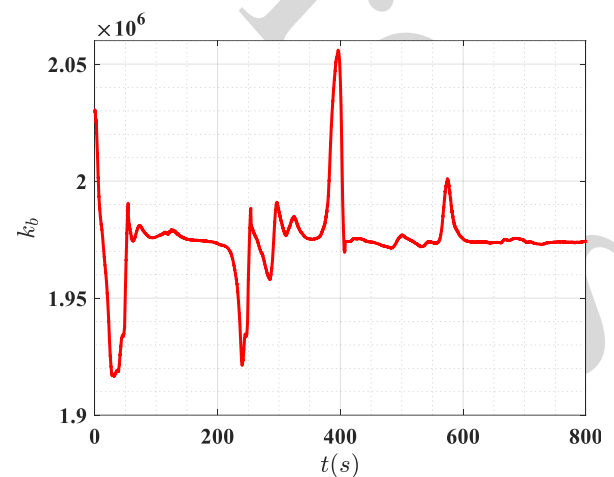


**Fig. 7.** The variation of  $k_b$  in the potential field method over time.

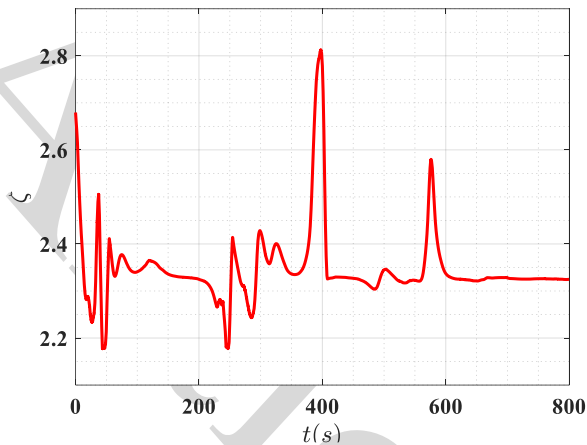


Fig. 8. The variation of  $\zeta$  in the potential field method over time.

Fig. 9, Fig. 10, Fig. 11 and Fig. 12 present 2D plots depicting the variation in distance to the first, second, third, and fourth obstacles over time, respectively. Each plot features a blue oscillatory curve that reflects changes in distance, showing dynamic interactions between the quadrotor and its surroundings. A red horizontal line is included as a minimum threshold, serving as a safety limit or collision boundary. The periodic behavior in the curves indicates moments when the UAV approaches obstacles, highlighting the method's responsiveness in maintaining a safe distance accordingly.

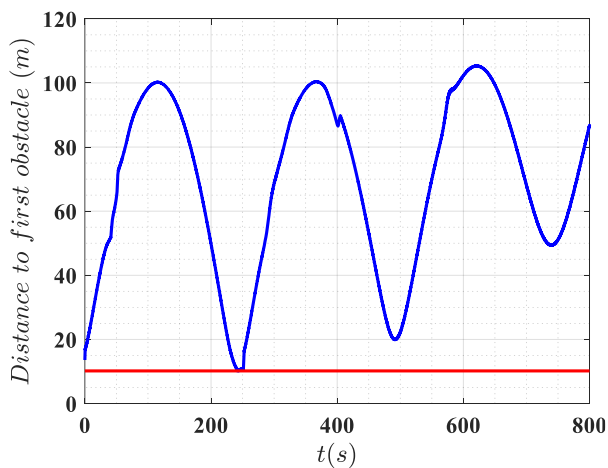


Fig. 9. Distance variation to the first obstacle over time.

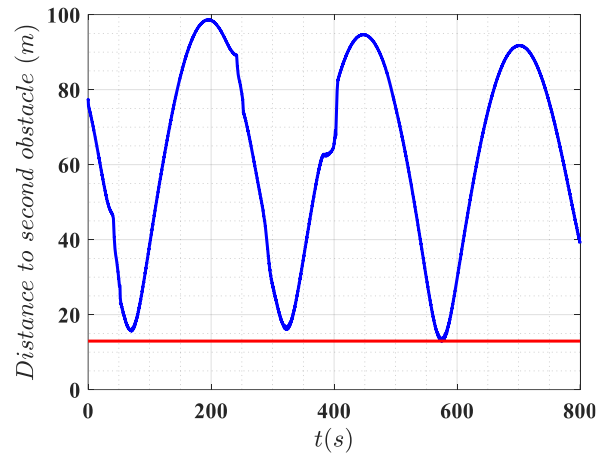


Fig. 10. Distance variation to the second obstacle over time.

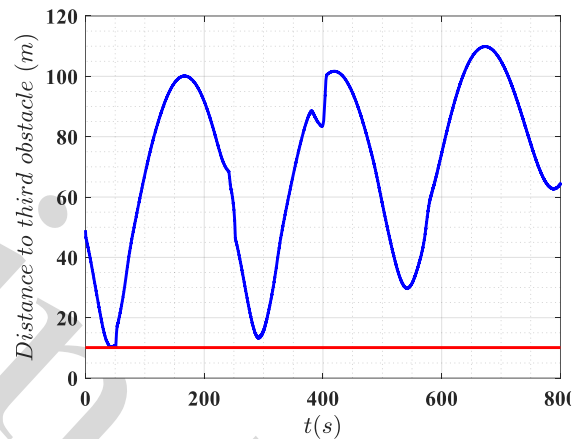


Fig. 11. Distance variation to the third obstacle over time.

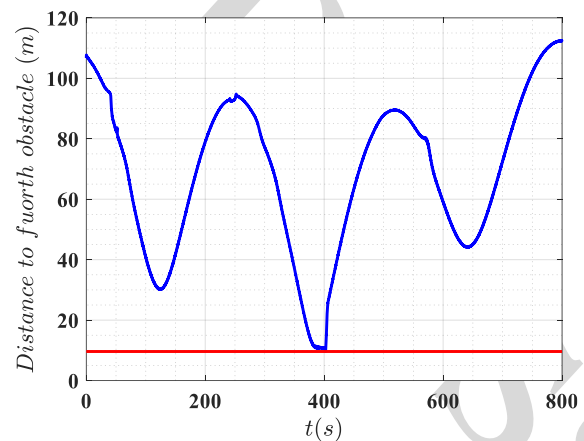


Fig. 12. Distance variation to the fourth obstacle over time.

## 8 Appendix

```
✓ Initialize simulation parameters
  •  $rx$  = Obstacle radius
  •  $nf$  = Obstacle radius scaling factors
  •  $V_{max}$  = Maximum voltage
  • Acceleration limits
  •  $dt$  = Time step
  •  $0 \rightarrow T$  = Simulation duration
  •  $\varphi_{max}$  = Maximum roll angle
✓ Generate nominal path
  •  $x_g, y_g$  and  $z_g$ 
✓ Set initial obstacle positions
  • Define initial positions
  • Assign dynamic velocities
✓ Initialize robot position
✓ Load fuzzy inference system
✓ Main simulation loop:
  • Evaluate fuzzy gains
  • For each obstacle:
 $d_{obs}$  = distance between the robot and obstacle
 $d_0 = rx \times nf$ 
  • Calculate repulsive force
  • If  $d_{obs} < d_0$ :
    Compute repulsive forces
  • else
    Set repulsive forces to zero
  • end
  • Calculate attractive force
  • Compute total forces
  • Considering wind effect
  • Apply constraints
  • Update robot position
  • Compute robot velocity, acceleration
  • Update obstacle positions
  • Update error values
 $e$  = nominal path - generated path
  • Normalize error values
✓ end
```

### CONFLICT OF INTEREST

The authors declare that they have no conflict of interest.

### REFERENCES

- [1] O. Khatib, "Real-time obstacle avoidance for manipulators and mobile robots," *The International Journal of Robotics Research*, vol. 5, no. 1, pp. 90-98, 1986, <https://doi.org/10.1177/027836498600500106>.
- [2] S. S. Ge and Y. J. Cui, "Dynamic Motion Planning for Mobile Robots Using Potential Field Method," *Autonomous Robots*, vol. 13, no. 3, pp. 207-222, 2002, <https://doi.org/10.1023/A:1020564024509>.
- [3] Y. Koren and J. Borenstein, "Potential field methods and their inherent limitations for mobile robot navigation," in *International Conference on Robotics and Automation*, Sacramento, California, vol 2, no. 1991, 1991, pp. 1398-1404.
- [4] X. Fan, Y. Guo, H. Liu, B. Wei, and W. Lyu, "Improved artificial potential field method applied for AUV path planning," *Mathematical Problems in Engineering*, vol. 2020, no. 1, 2020, Art. no. 6523158, <https://doi.org/10.1155/2020/6523158>.
- [5] L. Liu, B. Wang, and H. Xu, "Research on path-planning algorithm integrating optimization A-star algorithm and artificial potential field method," *Electronics*, vol. 11, no. 22, p. 3660, 2022, <https://doi.org/10.3390/electronics11223660>.
- [6] M. Wang, "Fuzzy logic based robot path planning in unknown environment," in *International Conference on Machine Learning and Cybernetics*, Guangzhou, China, 2005, vol. 2, pp. 813-818, <https://doi.org/10.1109/ICMLC.2005.1527055>.
- [7] P. Foehn, A. Romero, and D. Scaramuzza, "Time-optimal planning for quadrotor waypoint flight," *Science Robotics*, vol. 6, no. 56, 2021, Art. no. eabh1221, <https://doi.org/10.1126/scirobotics.abh1221>.
- [8] I. Shafieenejad, M. Siami Araghi, A. Sekhavat Benis, A. Mirzaee, and I. Fozouni Taloki, "Optimal path planning for autonomous space maneuvers based on reinforcement Q-learning and cubic network," *Journal of Technology in Aerospace Engineering*, vol. 6, no. 2, pp. 1-10, 2022, (in Persian), <https://doi.org/10.22034/jtae.2022.140118>.
- [9] I. Shafieenejad, M. R. Banitalebi Dehkordi, and M. A. Nourianpour, "A review of the application of optimization algorithms nature inspired in the design of flight paths," *Journal of Technology in Aerospace Engineering*, vol. 8, no. 3, pp. 75-98, 2024, (in Persian), <https://doi.org/10.22034/jtae.2024.8.3.6>.
- [10] R. Mahony, V. Kumar, and P. Corke, "Multirotor aerial vehicles: Modeling, estimation, and control of quadrotor," *IEEE Robotics and Automation Magazine*, vol. 19, no. 3, pp. 20-32, 2012, <https://doi.org/10.1109/MRA.2012.2206474>.

- [11] R. Omar, E. Sabudin, and C. K. M. CK, "Potential field methods and their inherent approaches for path planning," *ARPN Journal of Engineering and Applied Sciences*, vol. 11, no. 18, pp. 10801-10805, 2016.
- [12] M. Ghanifar, M. Kamzan, and M. Tayefi, "Intelligent tuning PID controller, simulation and comparison for a quadrotor," *Journal of Technology in Aerospace Engineering*, vol. 7, no. 4, pp. 23-33, 2023, (in Persian), <https://doi.org/10.30699/jtae.2023.7.4.3>.
- [13] W. Xie and J. Duan, "The design and simulation of fuzzy PID parameter self-tuning controller," *TELKOMNIKA Indonesian Journal of Electrical Engineering*, vol. 14, no. 2, pp. 293-297, 2015, <http://dx.doi.org/10.11591/telkomnika.v14i2.7674>.